Gulf and Caribbean Research

Volume 34 | Issue 1

2023

A Miocene Nannofossil Biostratigraphic Case Study: Alaminos Canyon Block 627 and Mississippi Canyon Block 555, and Sedimentation Rates in the Gulf of Mexico

Bethany L. Cobb Faulk
University of Alabama - Tuscaloosa, bcobbfaulk@gmail.com

Murlene W. Clark
University of South Alabama, mclark@southalabama.edu

Recommended Citation

Cobb Faulk, B. L. and M. W. Clark. 2023. A Miocene Nannofossil Biostratigraphic Case Study: Alaminos Canyon Block 627 and Mississippi Canyon Block 555, and Sedimentation Rates in the Gulf of Mexico. Gulf and Caribbean Research 34 (1): 79-88. Retrieved from https://aquila.usm.edu/gcr/vol34/iss1/13
DOI: https://doi.org/10.18785/gcr.3401.13

GULF AND CARIBBEAN

RESEARCH

Volume 34
2023
ISSN: 2572-1410

Published by

THE UNIVERSITY OF
SOUTHERN MISSISSIPPI

GULF COAST RESEARCH LABORATORY
Ocean Springs, Mississippi

Gulf and Caribbean Research Vol 34, 79–88, 2023
DOI: 10.18785/gcr.3401.13
Manuscript received October 5, 2022; accepted August 26, 2023

A MIOCENE NANNOFOSSIL BIOSTRATIGRAPHIC CASE STUDY: ALAMINOS CANYON BLOCK 627 AND MISSISSIPPI CANYON BLOCK 555, AND SEDIMENTATION RATES IN THE GULF OF MEXICO

Bethany Cobb Faulk[1,2*] and Murlene W. Clark[2]
[1]Department of Geological Sciences, University of Alabama, 201 7th Ave., Tuscaloosa, AL 35487 USA; [2]Department of Earth Sciences, University of South Alabama, 5871 USA Drive N. Mobile, AL 36688 USA; Corresponding author, email: bcobbfaulk@gmail.com

Abstract: The Miocene sediments of 2 deep–water boreholes from the northern Gulf of Mexico, from Alaminos Canyon (AC) Block 627 and Mississippi Canyon (MC) Block 555, have been biostratigraphically analyzed using calcareous nannofossils, revealing changes in sedimentation rates and depositional environments between these 2 areas. High nannofossil abundance values and low sedimentation rates generally recorded in the Alaminos Canyon region suggest a condensed section during much of the Miocene, associated with a basinal environment. Mississippi Canyon exhibits lower nannofossil abundance and higher sedimentation rates compared to Alaminos Canyon during the majority of the Miocene. Increased sediment volumes are largely attributed to input from the Mississippi River. Sedimentation rate was calculated for both sites. In the AC Block 627 borehole, sedimentation rate ranged from 13 to 107 m/million years (my), and in the MC Block 555 borehole, it varied from 11 to 914 m/my. One major anomaly was a low observed sedimentation rate in the lowest portion of the section at MC Block 555, in the interval defined between the extinctions of *Triquetrorhabdulus carinatus* and *Dictyococcites bisectus*. This may reflect a hiatus or possible fault which has shortened the section.

Key words: Deposition, basin, extinction, condensed, carbonate

Introduction

Calcareous nannofossil biostratigraphy is an underutilized resource with respect to sedimentation rate analysis in the literature of the Gulf of Mexico (GoM). Most borehole data are proprietary; therefore, the opportunity to analyze samples from 2 deep oil wells provides an important addition to the biostratigraphic database which has hither to been supplied by a nonspecific compendium of released proprietary data and Deep Sea Drilling Project (DSDP) sites located in the GoM.

During the Miocene, the primary locations of sediment discharge into the GoM were concentrated into a few deep structural embayments, which mostly overlapped with the placement of extant river systems (Blum et al. 2017, Xu et al. 2017). These expansive, low–gradient river systems created extensive, gently–sloping fans that reached hundreds of kilometers offshore (Blum et al. 2017).

During the early Miocene, the Edwards Plateau and Llano Uplift rose in Texas, supplying a higher volume of reworked sediments to the Rio Grande Embayment, which fed the Alaminos Canyon (AC) area (Galloway et al. 2000, Xu et al. 2017). It was during this period that the northwestern/central coast of the GoM had its most geographically extensive depositional centers. However, the extreme northeastern coast (directly upslope of the Mississippi Canyon (MC)) received low sediment volumes during this time (Galloway et al. 2000). According to the depositional mapping of Galloway et al. (2000), in the late early Miocene (ranging from slightly earlier than the Last Appearance Datum (LAD) of *Triquetrorhabdulus carinatus* to about the LAD of *Helicosphaera ampliaperta*), the northeast coast began receiving a slightly higher rate of sediment (Galloway et al. 2000).

Middle Miocene deposition is represented in the AC and MC study areas by the section ranging from the extinction of *H. ampliaperta* to the extinction of *Discoaster kugleri*. Together, the Central Mississippi River axis and East Mississippi River axis formed a large delta complex that extended the continental shelf up to 40 km (25 mi) during this time (Galloway et al. 2000). Erosion of the newly–rejuvenated Appalachian Mountains yielded a large supply of sediment to the eastern GoM (Xu et al. 2017). During the late middle to early late Miocene (c. LAD *D. kugleri* to c. LAD *Discoaster berggrenii*), the GoM experienced a significant regression in sea level which was terminated by a transgression in the latest Miocene. During the latest Miocene (post–LAD *D. berggrenii*), over 50% of the GoM was sediment starved.

The objective of this study is to biostratigraphically compare the Miocene section of 2 offshore boreholes in the GoM to evaluate differences in sedimentation rate between a condensed section offshore of southern Texas and a section south of Mississippi that, during the Miocene, was the site of dynamically–shifting depositional environments, which recorded contributions from the paleo–Mississippi River and MCAVLU clastic fans (Galloway et al. 2000). A comprehensive discussion of regional– to continental–scale GoM drainage and deposition is beyond the scope of this study. For a thorough analysis of these topics, the reader is referred to the publications of the GoM Basin Depositional Synthesis Project, led by the University of Texas Institute for Geophysics, particularly Galloway et al. (2000), Xu et al. (2017), and Fulthorpe et al. (2014).

Materials and Methods

Study area

The Bureau of Ocean Energy Management (BOEM) divides the U.S. Federal Waters ("Outer Continental Shelf") of the

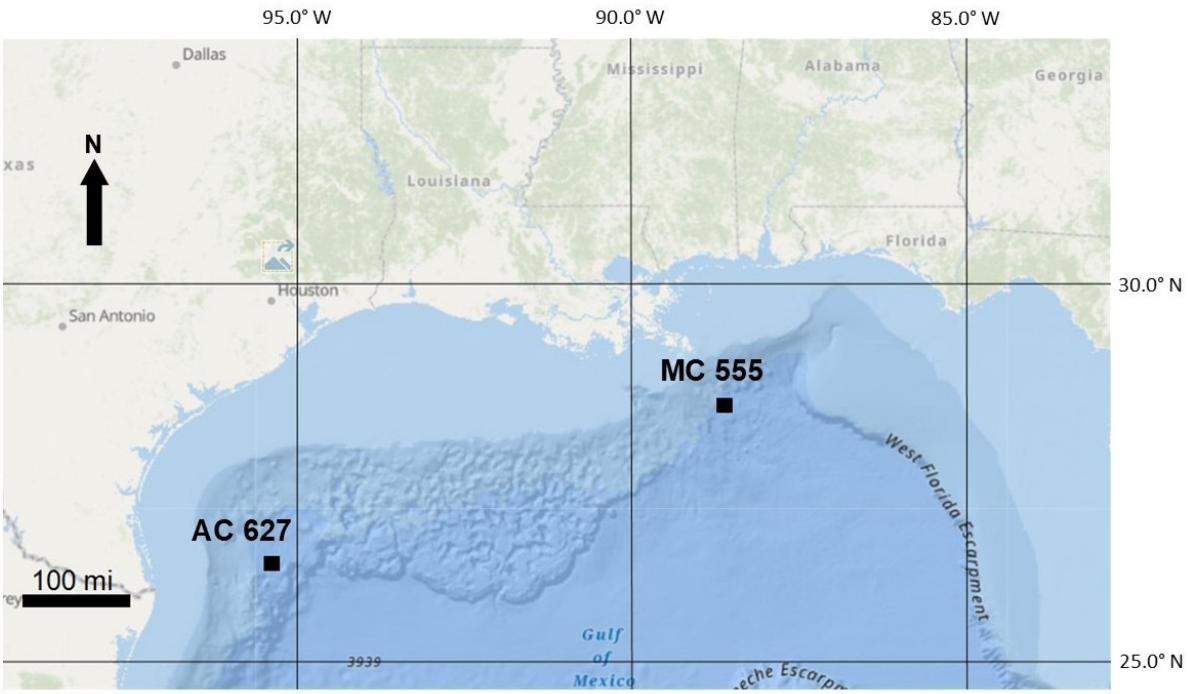

FIGURE 1. *Locator map of Alaminos Canyon (AC) Block 627 and Mississippi Canyon (MC) Block 555 in the northern Gulf of Mexico. Base map by marinecadastre.gov.*

GoM into regions, typically named for a prominent geologic feature within their borders, which facilitates leasing for oil and gas exploration. These regions are subdivided into numbered blocks. The first borehole in this project is from Alaminos Canyon Block 627 (AC 627; 26.3° N, 95.4° W; BOEM 2014), located off the eastern coast of southern Texas (Figure 1). AC 627 is situated west of Alaminos Canyon, the most prominent feature in the region, and the one for which it was named. Alaminos Canyon is a north—south trending submarine canyon (Bouma et al. 1968) cut into the western end of the Sigsbee Escarpment, a defining bathymetric feature of the GoM. The Sigsbee Escarpment is a salt front formed from the downdip migration of the Jurassic Louann Salt Formation. Alaminos Canyon may have formed from converging salt fronts originating from 2 different basins, or by turbidity currents with subsequent alteration by salt diapirism (Uchupi 1975).

The AC 627 borehole was drilled in about 2 km of temperate water (Poag 2015), which is above the calcite lysocline (Haq 1998). Accordingly, nannofossils at this site have experienced little dissolution and are well—preserved. The water mass above AC 627 is not significantly affected by any modern currents or upwellings (Poag 2015). Presently, AC 627 lies beneath relatively still, isolated, deep water. The AC 627 borehole represents a condensed section during much of the Miocene and shows evidence of high carbonate deposition and relatively little influx from clastic sediments. During the middle Miocene, AC 627 was located in the Corsair Apron, which was fed by the Corsair River axis and the Norias River axis. This fan system extended the continental margin by over 50 km (30 mi) (Galloway et al. 2000). The deltas supplying AC 627 had greatly shifted landward during the late middle to early late Miocene, leaving AC 627 in the northernmost distal toe of the Western Gulf Apron (Galloway et al. 2000). The clastic fans had fully shifted away from AC 627 during the latest Miocene, leaving it in a basin depositional environment.

The second offshore borehole examined in this study is from Mississippi Canyon Block 555 (MC 555; 28.4° N, 88.6° W; BOEM 2000). Mississippi Canyon is one of the most pronounced features of the northern GoM (Goodwin and Prior 1989, Hart et al. 2008). It is the present conduit delivering sediment from the Mississippi River drainage basin to the deeper GoM (Hart et al. 2008) and is a site of historically high levels of clastic riverine sedimentation. Carbonates compose less than 1% of total sediment in the canyon (Ross et al. 2009). During the middle Miocene, the MC 555 borehole location was situated in a basin. The Mississippi delta complex narrowly bypassed MC 555 to its west, and the large MCAVLU sediment fan bypassed it to the east, each by a narrow margin. During the late middle to early late Miocene, MC 555 was situated on the easternmost side of a sandy shelf derived from the Mississippi delta system. MC 555 was located solidly within the sandy shelf fed by the Mississippi delta system during the latest Miocene (Galloway et al. 2000).

Abundance and preservation

Biostratigraphic analysis included abundance estimates for over 50 individual nannofossil taxa, as well as overall abundance of the assemblage. Reworked species were also tracked as a group. Here, we consider reworked specimens to be from any species that went extinct prior to the Miocene. This group was predominantly composed of Cretaceous taxa in our slides. Hay's (1970) system was employed to record the abundance of each individual taxon found while zoning, and is organized

TABLE 1. *Hay's (1970) nomenclature for abundance of individual taxa. FOV = field of view.*

Abbreviation	Meaning	Number of specimens in FOV
V	Very abundant	> 10
A	Abundant	1-10
C	Common	1 per 2-10 FOV
F	Few	1 per 11-100 FOV
R	Rare	1-2 per slide

TABLE 2. *Bergen's (1984) nomenclature for abundance of overall assemblage. FOV = field of view.*

Abbreviation	Meaning	% of the FOV covered by nannofossils
A	Abundant	Over 50%
C	Common	10-50%
F	Few	1-10%
R	Rare	<1%
B	Barren	Void of nannofossils

as shown in Table 1. To measure the abundance of the entire assemblage, Bergen's (1984) system was utilized, as shown in Table 2.

Biostratigraphy

Offshore boreholes AC 627 and MC 555 were investigated via prepared slides provided by Paleo Data, Inc., an industrial biostratigraphic firm operating widely in the GoM, which is now owned by PetroStrat Ltd. Access to this resource afforded an unusual opportunity to examine the Miocene biostratigraphy of deep—water sediments in the GoM. These particular sites were requested due to the expectation of a complete Miocene section.

Slides were examined using a 1500 power Olympus BH2 binocular light microscope with a PO 100 oil immersion lens and wide field 15x eyepieces. Smear slides were made using a technique by which nannofossils were concentrated by timed settling intervals. Drops of suspended sediment were mounted on a coverslip and dried. The coverslip was then mounted on a glass slide with Norland 61 optical adhesive.

Because cuttings are employed instead of cores, only extinctions and acmes are viable biostratigraphically. This is because contamination is inevitable due to the small size of nannofossils, rendering origination depths unreliable. Downhole caving occurs, and drilling mud contaminates new samples, making nannofossils appear lower in the section than their true inceptions.

The zonation scheme used in this project is the most recent biostratigraphic scheme published by Paleo Data, Inc. at the time of this writing: Biostratigraphic Chart — Gulf Basin, USA Quaternary and Neogene Ver. 1701 (Paleo Data, Inc. 2017). Eighteen Miocene index species are used in this study, and micrographs of each species are shown in Figure 2:

Discoaster quinqueramus Gartner 1969
Discoaster berggrenii Bukry 1971
Discoaster calcaris Gartner 1967
Discoaster loeblichii Bukry 1971
Catinaster mexicanus Bukry 1971
Discoaster prepentaradiatus Bukry and Percival 1971
Discoaster bollii Martini and Bramlette 1963
Discoaster hamatus Martini and Bramlette 1963
Catinaster calyculus Martini and Bramlette 1963
Catinaster coalitus Martini and Bramlette 1963
Coccolithus miopelagicus Bukry 1971
Discoaster kugleri Martini and Bramlette 1963
Sphenolithus heteromorphus Deflandre 1953
Helicosphaera ampliaperta Bramlette and Wilcoxon 1967
Sphenolithus belemnos Bramlette and Wilcoxon 1967
Discoaster calculosus Bukry 1971
Triquetrorhabdulus carinatus Martini 1965
Dictyococcites bisectus (Hay, Mohler and Wade 1966) Bukry and Percival 1971.

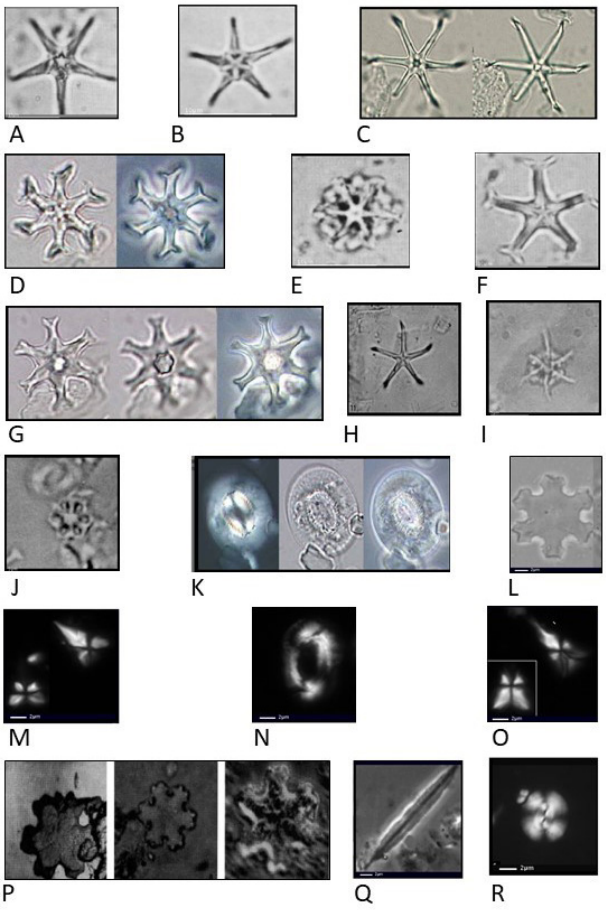

FIGURE 2. *Micrographs of the 18 indicator species used in this study. A. Discoaster quinqueramus B. Discoaster berggrenii C. Discoaster calcaris D. Discoaster loeblichii E. Catinaster mexicanus F. Discoaster prepentaradiatus G. Discoaster bollii H. Discoaster hamatus I. Catinaster calyculus J. Catinaster coalitus K. Coccolithus miopelagicus L. Discoaster kugleri M. Sphenolithus heteromorphus N. Helicosphaera ampliaperta O. Sphenolithus belemnos P. Discoaster calculosus Q. Triquetrorhabdulus carinatus R. Dictyococcites bisectus (Reticulofenestra bisecta). Images compiled from mikrotax.org. Image sources: (A, B, E, F) Theodoridis 1984; (C) Browning et al. 2017; (D, G, K) Salomon 1999; (H, I, J) Martini and Bramlette 1963; (L, M, N, O, Q) Young 1998; (P) Bukry 1971; (R) Bown 2005.*

In AC 627, the Miocene section started at 2,573 m (8,440 ft) below the GoM seafloor and terminated at 3,158 m (10,360 ft), encompassing a total of 585 m (1,920 ft) of sediment. At MC 555, the section spanned depths of 3,325 m (10,850 ft) subseafloor to 7,001 m (22,970 ft), covering 3,694 m (12,120 ft) in total. In each borehole, slides were prepared at depth increments of 9.1 m (30 ft). An exception is in the earliest part of MC 555, in which the slides were processed at 3.1 m and 6.1 m (10 ft and 20 ft) intervals. This only applies to a few slides and is marked accordingly in Table 4. The entire Miocene section of each borehole was analyzed; however, due to the extreme sedimentation rates encountered at MC 555, the slides were examined at different intervals in each section.

The AC 627 slides were analyzed at an interval of 27.4 m. An apparent extinction for an index species occurs the first time that the species is encountered downhole. When the apparent extinction of an index species was found using 27.4 m intervals, it was further refined by individual slides, which made the extinction horizon accurate to within 9.1 m. Starting at the apparent extinction, slides were analyzed receding upwards by 9.1 m intervals until the index species could no longer be observed. This is considered to represent the LAD. Some slides did not lend themselves to abundance estimations due to severe clumping issues that occurred when the slides were created. In the cases where a slide needed to be analyzed for an index species' LAD, the species was marked P for Present when it was located. Where the species could not be found, it was marked NP for Not Present.

The MC 555 site contained a significantly thicker Miocene section than that observed at AC. As such, its abundance values were analyzed every 146 m (480 ft), from youngest (top) to oldest (bottom) material. When an apparent extinction was found within a 146 m interval method, it was further refined into smaller intervals, making the LAD depth more accurate. Abundance was not kept for these refining slides. Rather, index species on these slides were marked P and NP, as defined above. The vertically highest slide in which the species is marked Present is considered to be the LAD.

Sedimentation rates were calculated using the geochronology of Anthonissen and Ogg (2012) or, where markers were not recognized by Anthonissen and Ogg (2012), by the dates of Paleo Data, Inc. (2017). The absolute ages listed are those of Anthonissen and Ogg (2012) supplemented by *C. mexicanus* and *D. prepentaradiatus*, datums routinely used in the GoM by Paleo Data, Inc. (2017). The dates between index species' extinctions were compared to their depths to generate sedimentation rates throughout time for each borehole.

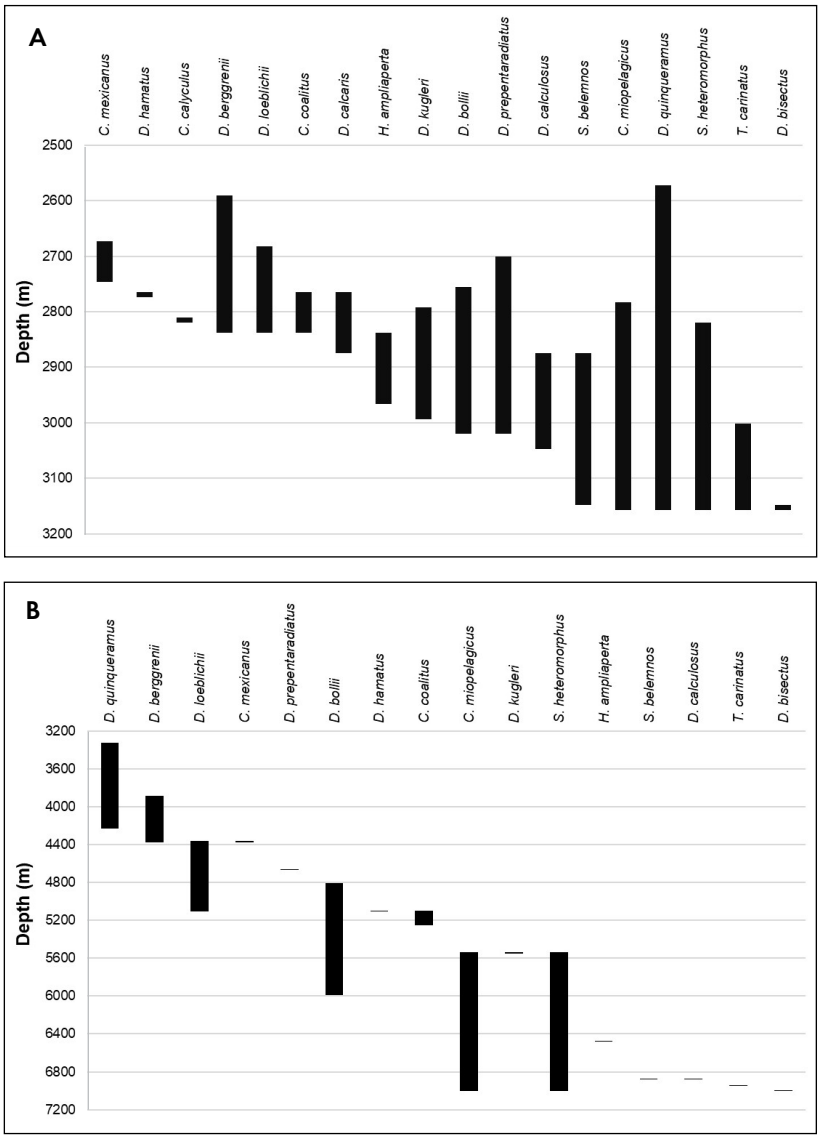

FIGURE 3. *Depth range chart for index species. First Appearance Datums (FADs) are only approximate due to the use of cuttings. A. Alaminos Canyon Block 627 borehole. B. Mississippi Canyon Block 555 borehole.*

Results

A total of 585.2 m (1,920 ft) of sediment was examined for nannofossils at AC 627. Biostratigraphic and abundance data for all 54 taxa examined for this site are recorded in Table 3. This site is highly concentrated with nannofossils; in fact, all slides except 2 were marked as *Abundant*. In all except the latest Miocene (c. the LAD of *Catinaster calyculus*), reworked Cretaceous nannoflora were fairly prevalent (one fossil per 2 or more fields of view). Post—*C. calyculus*, reworked species were still present, although in fewer numbers (*Few* to *Rare*). A range chart was created for the index species at this well (Figure 3A). The inceptions (First Appearance Datums, or FADs) are only approximate since cuttings were the source of the samples.

A total of 3,694 m (12,120 ft) of sediment was analyzed for MC 555. Table 4 displays the biostratigraphic and abundance data for all 54 taxa examined for the MC borehole. There was a marked difference in the abundance of fossils present in MC 555 compared to AC 627. The amount of reworking of former species was highly variable, although it follows a loose trend of decreasing upward. Figure 3B shows the range chart of the index taxa at this location. Again, the FADs here are only approxi-

TABLE 3. *Abundance Data for Borehole AC 627. V = Very Abundant, A = Abundant, C = Common, F = Few, R = Rare, B = Barren, P = Present, NP = Not Present. "Reworked" is the collective term for any specimens whose species went extinct prior to the Miocene.*

Range (m)	Total nannofossil abundance	*Helicosphaera kamptneri*	*Helicosphaera sellii*	*Calcidiscus mcintyrei*	*Calcidiscus leptopora*	*Syracoshpaera spp.*	*Umbilicosphaera spp.*	*Rhabdosphaera spp.*	*Reticulofenestra small*	*Reticulofenestra spp.*	*Reticulofenestra pseudoumbilica*	*Pontosphaera japonica*	*Pontosphaera discopora*	*Pontosphaera multipora*	*Pontosphaera spp.*	*Ceratolithus cristatus*	*Ceratolithus spp.*	*Watznaueria spp.*	*Scyphosphaera spp.*	*Sphenolithus spp.*	*Sphenolithus abies*	*Discoaster triradiatus*	*Discoaster brouweri*	*Discoaster pentaradiatus*	*Discoaster variabilis*	*Discoaster surculus*	*Discoaster asymmetricus*	*Coccolithus pelagicus*	*Amaurolithus tricorniculatus*	*Amaurolithus delicatus*	*Ceratolithus acutus*	*Discoaster quinqueramus*	*Discoaster berggrenii*	*Discoaster calcaris*	*Discoaster loeblichii*	*Catinaster mexicanus*	*Discoaster prepentaradiatus*	*Discoaster bollii*	*Discoaster bellus*	*Discoaster hamatus*	*Catinaster calyculus*	*Catinaster coalitus*	*Coccolithus miopelagicus*	*Discoaster kugleri*	*Cyclicargolithus floridanus*	*Sphenolithus heteromorphus*	*Discoaster petaliformis*	*Helicosphaera ampliaperta*	*Sphenolithus belemnos*	*Discoaster calculosus*	*Braarudosphaera spp.*	*Triquetrorhabdulus carinatus*	*Helicosphaera truncata (recta)*	*Dictyococcites bisectus*	Reworked
2573-2582	A	A			C	R		F	V	V	C		C	C		R		R	F		V	R	A	A	C	C		C		R	F	R																							R
2582-2591	A	A		R	A	F	A	R	V	V	C		F	F		R	R		F		V		A	A	C	C		C				F																							F
2591-2600	A	A			C	F	R	R	V	V	C	F	F	F		R		R	F		V	R	A	A	C	C		C			R	A	F																						
2600-2609	A	A		R	C		F	R	V	V	C		F	F	F	R			F		V	R	C	C	C	F		C			R	A	R																						
2627-2637	A	A	R		C		F	R	V	V	C		F	F					R		V		C	C	C	C		A			R	A	C																						F
2655-2664	A	A		F	C	F	A		V	V	F	F	F	F	R		R	R	F		V	R	C	F	C			A		R		C	A																						F
2673-2682	A	A		F	A	F	C	R	V	V	R		F	F				R	R	R	V		C	C	C			A				R	A		NP	R							R												F
2682-2691																																			P																				
2691-2701																																																							
2701-2710																																					P																		
2710-2719	A	A		R	A		C		V	A	R	R	R	F					R		A	R	A	C	C			A					A		R	F							R												R
2737-2746	A	C		R	C		C	R	A	A	F		R	F				R		F	A	R	A	F	C			A				F	F		R	R	F																		F
2755-2765	A	C		R	C	F	C		V	A	C	R	R	F	R						A		C	F	C			A					C		R			F	F																F
2765-2774	A	C			A		R	R	V	V	C		R	F							A		C	C	C	R	R	A				R	F	R	R			F	F	R		R													F
2774-2783	A	C			C		C		V	C	C	R	R	R					R		A		A	R	C		R	A					R					F	C																R
2783-2792	A	C			C		C	R	V	A	C	F		F							A	R	C	R	C			A										F	F			R	R												R
2792-2801	A	F		F	C		F	R	V	A	C		R	F				R			A	R	C	R	C		R	A				R					R	F	F				F	R											R
2801-2810	A	C		R	F	R	C	R	V	A	C	F	R	F				R			C		C	R	F		R	A				R	R				R	F	F				F	F											F
2810-2819	A	C		R	R	R	F	R	V	A	F		R	F			R	R			A		A	R	R		R	A				R			R		R	F	C		R	R	C	F	R										F
2819-2829	A	C		R	C		C	R	V	A	F	R	R	F				R	R		A		C	R	C			A				C	C		R			R	F			F	F	R	R	R									C
2829-2838	A	A			R		C		V	V	F	R	R	F				F			A		C	R	A			A				R	R		R		R	F	R			R	C	F	F	F	R								F
2838-2847	A	C			R		C	R	V	V	F			F				F			A		C		C			A				R					R	F	R				F	F	C	F	R	R							F
2847-2856	A	C			R		C		V	V	F		R	F							A		C	R	F		R	A										F	F				F	C	C	F	R								C
2865-2874	C	A			F		F		V	V	F	R		F				F	R		C		C	R	C			A				R		R			R	C	F				C	F	C	F									R
2874-2883	A	C			R		C	R	V	A		R		F				F			A		F	R	F			A				R						C	R				F	F	A	C	R	R	R	R	R				F
2902-2911	A	A					C		V	A			R	F				F			A		C		F			A				R					R	F	R				C	F	A	C			R						F
2929-2938	A	A			R	R	C		V	A	F			F				F			A		F	R	F			A				R						F					C	F	A	C			F	R					C
2957-2966	A	F			F		C		V	A	R		R	F				F			A		F		F			A				R					R	R	R				F		V	F	R	R	F						C
2984-2993	A	C			R		F	R	V	A	R	R		F				F		F	A		R	F	F		R	A				R						R	R				F	R	V	F			F	R					C
2993-3002	A	C			R	R	F		V	A	R	R	R	F				R			A		R		R			A															F		V	F			F						F
3002-3011	A	C					F	R	V	A	R			F				F			A		R	F	R			A				R	R										C		V	F			F			R			C
3011-3021	A	C					C		V	A			R	F				F		F	A		R		F			A									R	R					F		V	F			R			R			C
3039-3048	A	C		R	R		F		V	A	R			C				F			A		R	F	R			C				R											F		A	R				R					C
3057-3066	A	F			R		F		V	A	F	R	R	F				C			A			R				C															C		A	F			R						C
3066-3075	C	C		F	R		A		V	A	F		R	F				C			A			F				C									R	R					F		A	R		R					R		C
3094-3103	A	C					F		V	A	R			F				C			A				R			A				R										R	C		A	F			R			R			F
3121-3130	A	C					F		V	A	F		R	F				C			A							C															C		A	F			R		R				F
3139-3149	A	C					F		V	A	F			F	R			C			A			R				A				R											C		V	F			F			F			F
3149-3158	A	C				R	F		V	A	R			F	R			C			A			F				A				R											C	R	V	F						F	R	R	F

TABLE 4. *Abundance Data for Borehole MC 555. V = Very Abundant; A = Abundant; C = Common; F = Few; R = Rare; B = Barren; P = Present; NP = Not Present. "Reworked" is the collective term for any specimens whose species went extinct prior to the Miocene.*

Range (m)	Total nannofossil abundance	*Helicosphaera kamptneri*	*Helicosphaera sellii*	*Calcidiscus mcintyrei*	*Calcidiscus leptopora*	*Syracosphaera spp.*	*Umbilicosphaera spp.*	*Rhabdosphaera spp.*	*Reticulofenestra small*	*Reticulofenestra spp.*	*Reticulofenestra pseudoumbilica*	*Pontosphaera japonica*	*Pontosphaera discopora*	*Pontosphaera multipora*	*Pontosphaera spp.*	*Ceratolithus cristatus*	*Ceratolithus spp.*	*Watznaueria spp.*	*Scyphosphaera spp.*	*Sphenolithus spp.*	*Sphenolithus abies*	*Discoaster triradiatus*	*Discoaster brouweri*	*Discoaster pentaradiatus*	*Discoaster variabilis*	*Discoaster surculus*	*Discoaster asymmetricus*	*Coccolithus pelagicus*
2457-2466	A	A		C	A	F	C	F	V	V		R	F			F		R	F				A	C			F	C
3307-3316																												
3316-3325																												
3325-3344																												
3344-3353	C	C		R	R		R		A	A	F		R					R		R	A			F				F
3490-3499	R	R							R	F											F			R				R
3636-3645	B																											
3783-3792	R	R							F	F								C			F							
3856-3865																												
3883-3892																												
3892-3901																												
3929-3938	C	C			F				V	A		R	R	F						R	A		F	F	F			C
4075-4084	R								C	R											F							F
4221-4231	C	F			F		R		V	C				R				R			A		C	R	R			C
4331-4340																												
4349-4359																												
4359-4368																												
4368-4377	F	F			F	R	F		A	C								F			A		F	R				F
4514-4523	F	R			R				C	R								F			C							F
4660-4670	F	C		R	C		C		C	C	F										A		C		F			A
4807-4816	C	C			F		F			A					R			F			F		C		R		R	A
4953-4962	C	F			R				C	A	F							F			R		F		R			C
5099-5108	C	A			F				V	A	F		F	F				R			C		F		F		R	C
5246-5255	C	C			R		R		V	A	R			R				F			C				R			C
5392-5401	F	R							C	C	R							C			R							
5538-5547	A	C			R		F		A	A				R						R	A		R		F			A
5685-5694	C	F							C	C								A		F	F							F
5831-5840	F	R							C	C	R			R				C			R							F
5977-5986	C	F							C	C	R							F			C							C
6123-6130	C	C							C	C					R						C		R					A
6270-6276	F	R							R	F								R										R
6416-6422	C	F							C	R								C										R
6477-6483																												
6559-6565	F	F							C	C								F			R							F
6706-6712	C	C							A	A			R	F				F			F							A
6852-6858	C	C							R	F									R		R							A
6870-6876																												
6943-6949																												
6998-7001	C	C								R											R							F

Range (m)	*Amaurolithus tricorniculatus*	*Amaurolithus delicatus*	*Ceratolithus acutus*	*Discoaster quinqueramus*	*Discoaster berggrenii*	*Discoaster calcaris*	*Discoaster loeblichii*	*Catinaster mexicanus*	*Discoaster prepentaradiatus*	*Discoaster bollii*	*Discoaster bellus*	*Discoaster hamatus*	*Catinaster calyculus*	*Catinaster coalitus*	*Coccolithus miopelagicus*	*Discoaster kugleri*	*Cyclicargolithus floridanus*	*Sphenolithus heteromorphus*	*Discoaster petaliformis*	*Helicosphaera ampliaperta*	*Sphenolithus belemnos*	*Discoaster calculosus*	*Braarudosphaera spp.*	*Triquetrorhabdulus carinatus*	*Helicosphaera truncata (recta)*	*Dictyococcites bisectus*	Reworked
2457-2466																											R
3307-3316				NP																							
3316-3325				NP																							
3325-3344				P																							
3344-3353				F											F												
3490-3499																											
3636-3645																											
3783-3792																											F
3856-3865					NP																						
3883-3892					P																						
3892-3901					P																						
3929-3938				C	F																		R				
4075-4084																											
4221-4231				F	A																						
4331-4340						NP	NP	NP																			
4349-4359							NP	NP																			
4359-4368							P	P																			
4368-4377					C		R	R																			F
4514-4523																											F
4660-4670									R														R				
4807-4816										C	F																R
4953-4962										C	F																F
5099-5108							R			C	F	R		R			R										
5246-5255										C	R			F									R				F
5392-5401																							R				C
5538-5547										F					C	R	R	R					R				R
5685-5694																	R										A
5831-5840																											C
5977-5986										R					R												C
6123-6130															F			R									F
6270-6276															R												
6416-6422																	R										C
6477-6483																				P							
6559-6565															R		R	F									R
6706-6712															C		A	C									
6852-6858															C		A	C					R				
6870-6876																						R					
6943-6949																								R			
6998-7001															C		C	C								R	

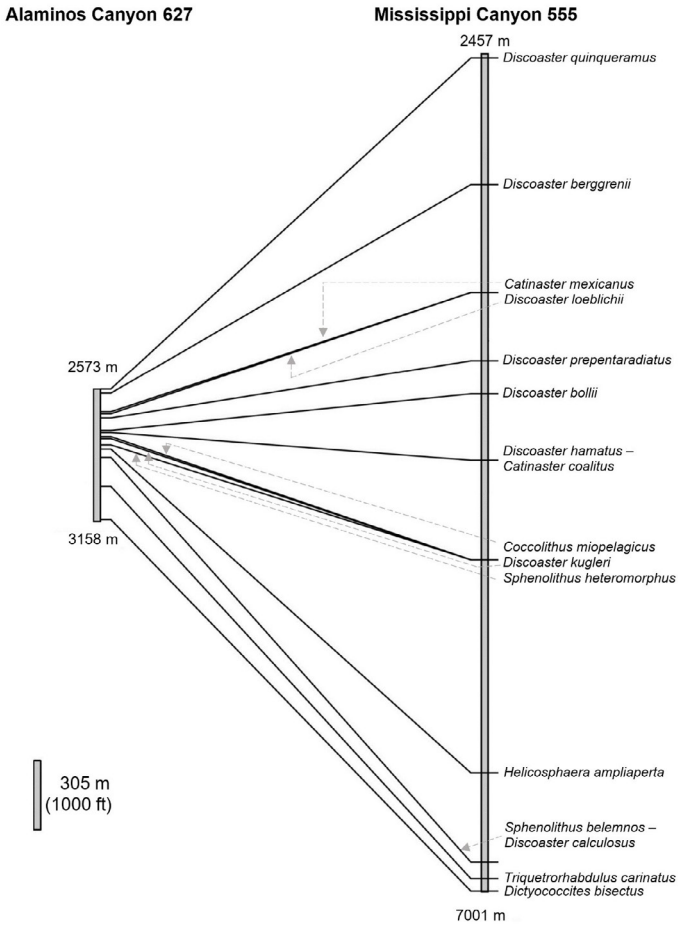

FIGURE 4. *Graphical comparison of Last Appearance Datums (LAD) depths for index taxa at AC 627 and MC 555. Solid lines connect the same bioevent in each well, and dashed lines clarify which solid line is being referred to where LADs co-occur in MC 555 but not AC 627.*

mate. A comparison linking the extinctions of index species between AC 627 and MC 555 is shown in Figure 4. *Discoaster calcaris* and C. *calyculus* could not be found in MC 555, so they had to be dropped from the final analysis.

TABLE 5. *Ages and depths of Last Appearance Datums (LAD) of apropos index taxa in AC 627 and MC 555. Sedimentation rates calculated from these data are shown graphically in Figure 5. Ages are from Anthonissen and Ogg (2012) and Paleo Data, Inc. (2017). Ma = millions of years ago.*

Index taxon	LAD Age (Ma)	LAD Depth (m) AC 627	LAD Depth (m) MC 555
Discoaster quinqueramus	5.59	2,573	3,325
Catinaster mexicanus	8.05	2,673	4,359
D. prepentaradiatus	8.70	2,701	4,660
D. bollii	9.21	2,755	4,807
D. hamatus	9.53	2,765	5,099
D. kugleri	11.58	2,792	5,538
Helicosphaera ampliaperta	14.91	2,838	6,477
Triquetrorhabdulus carinatus	18.28	3,002	6,943
Dictyococcites bisectus	23.13	3,149	6,998

Table 5 gives the LAD ages and depths of selected index species throughout the Miocene. The index taxa in Table 5 have proven to be the most reliable from which to calculate comparative sedimentation rates between the 2 sites in our study. Other index species tabulated in the abundance analysis were found to be less reliable in AC 627 and MC 555 due to occurrence out of temporal sequence with respect to depth, or due to co—occurrence at the same depth interval, perhaps as an artifact of sampling frequency, especially when the time separation between the species is small. These have been omitted from Table 5. Sedimentation rates calculated from the ages and depths of Table 5 are summarized graphically in Figure 5. It is apparent from Figure 5 that MC 555 preserves a much higher sedimentation rate than AC 627 during all but the earliest interval of the Miocene (between the LAD of *D. bisectus* at 23.13 Ma and the LAD of *T. carinatus* at 18.28 Ma).

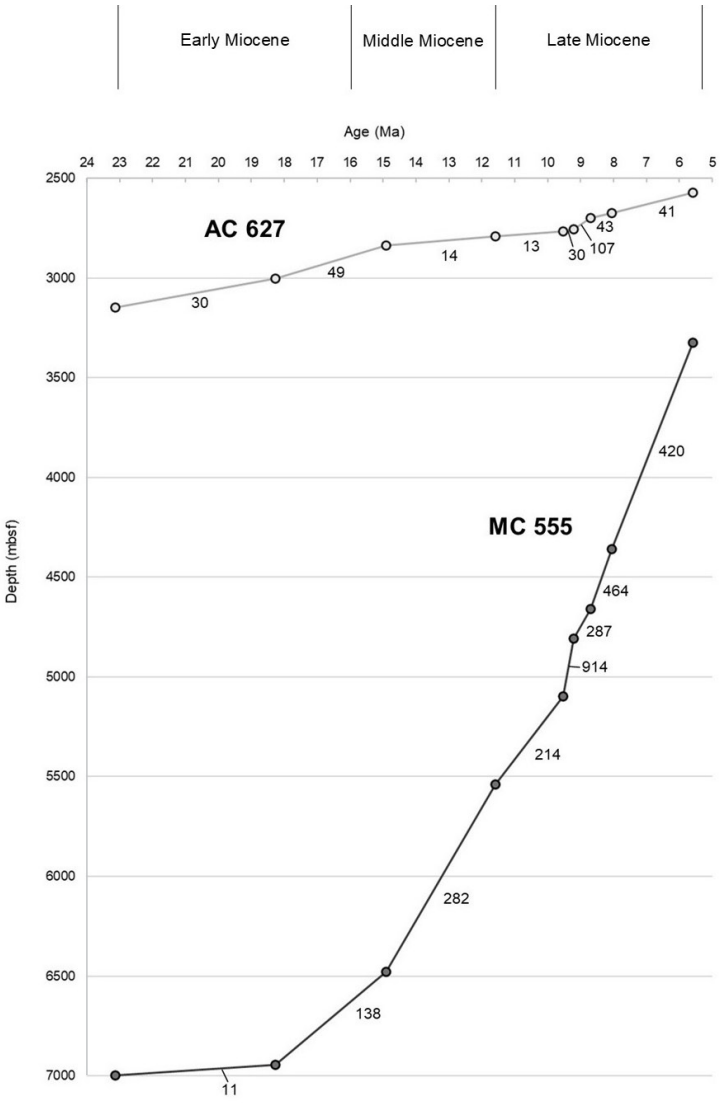

FIGURE 5. *Sedimentation rates through time at AC 627 and MC 555, calculated using the index species extinctions of Table 5. The rates are the numbers below each line segment, in m/million years. Ma = millions of years ago; mbsf = meters below seafloor.*

Discussion

The section at AC 627 is, for the most part, a condensed section. There is a distinctively high abundance of reworked species in this borehole. This could be attributed to the uplift of the Edwards Plateau in Texas (Galloway et al. 2000). This might also explain why a similar spike in reworked species is not observed in the MC borehole: MC 555 was fed by different watersheds than the ones delivering Edwards Plateau sediments to the GoM. In the lowest part of MC 555 (between *T. carinatus* LAD and *D. bisectus* LAD), sedimentation rate is 11 m/my, which is an order of magnitude less than the next highest sedimentation rate in its Miocene history (i.e., the interval immediately following). This much—shortened interval represents the most significant anomaly present in either section. This may represent a hiatus from non—deposition due to MC 555's basinal location (Galloway et al. 2000). Alternatively, this may support evidence for a fault in the area. Faults may be associated with the hypersubsidence of the early Miocene GoM basin. The biostratigraphic analysis of more wells in the area would better resolve the cause of this shortening. In the second half of the early Miocene, the slightly increased sedimentation volume to the MC 555 area (Galloway et al. 2000) is observable in the biostratigraphic data. It becomes noticeable post—*Sphenolithus belemnos* and *D. calculosus* extinctions, and apparently continues through the end of *H. ampliaperta*'s range.

In the middle Miocene, the AC 627 borehole does not appear to reflect the overall regional trend of high sediment accumulation due to the Corsair fan, as it is a condensed section for this time. Without further inquiry it cannot be known why clastic sediment accumulated so slowly during the middle Miocene in this section. It could perhaps be due to a localized influence such as sediment bypass. The MC 555 borehole also does not reflect its overall regional depositional trend, a basin. Rather, the biostratigraphic data provides evidence of substantial clastic sediment input during the middle Miocene. This is not entirely surprising, considering it is surrounded on every side by massive regions of clastic sediment accumulation. This high sedimentation rate may be due to a localized factor. An example may be that MC 555 was a bathymetric lowstand. Whatever the case may have been, MC 555 has an excessively large middle Miocene interval relative to AC 627.

In the late middle to early late Miocene, as in the middle Miocene, AC 627 was again in a regional trend of clastic deposition but is still preserved as a condensed section. MC 555 was fully located within the Gulf Central Apron at this point, supplied by ample clastics from the prolific Mississippi axes (Galloway et al. 2000). Accordingly, it forms a long section for this depositional episode.

In the latest Miocene, AC 627 had fully emerged from the clastic depositional areas and into a basin, which appears to agree with its condensed nature. MC 555 was fed high volumes of sediment by the Mississippi River (Galloway et al. 2000), which is also in agreement with its long sediment section during this time.

Overall, MC 555 has a much longer Miocene section, due to its placement downslope of the Mississippi River delta system (Galloway et al. 2000). During the last half of the Miocene, the sedimentation rates at MC 555 were notably greater than at AC 627. In the first half, however, in the interval defined between *S. belemnos* LAD and *D. bisectus* LAD, the rates were similar between the wells. Overall, the Mississippi Canyon Miocene section is approximately 6 times the thickness of the Alaminos Canyon section.

Some complications arose due to the observation interval in MC 555. Ultimately, it was determined that examining slides every 146 m was too coarse an interval to use. Several index species' ranges were so brief that they were entirely missed via this method and could only be found via extensive refinement. Using a smaller interval for similar wells would yield greater results in pinpointing index ranges more readily. It is also probable that since so many index species were overlooked initially through the use of 146 m increments, many nuances in assemblage abundance were not detected. While index species in AC 627 remained consistently *Abundant*, those in MC 555 ranged from *Rare* to *Abundant*. This wide variation might be attributed to the sediment load from the Mississippi River, especially during periods when MC 555 was contained within the Mississippi delta's clastic aprons (the latter half of the Miocene). Despite the inability of our initial choice of interval to better refine several extinction horizons, it is accurate enough to be useful in observing overall sedimentation rate trends. No problems were identified with the 27 m increment associated with AC 627. Due to the shortness of the section, index biohorizons were identified within an accuracy of 9.1 m after refinement.

Analysis of AC 627 and MC 555 demonstrates the powerful functionality and continued relevance of nannofossil biostratigraphy in the geologic inquiry of the GoM. In the case of the AC 627 and MC 555 wells, nannofossils allow the determination of a precise age control of sediments buried thousands of meters below the modern seafloor. From this, nannofossils permit the calculation of sediment rates, even for rock units with homogenous lithology. This enables great insight into the processes of ancient earth environments, both marine and terrestrial.

Acknowledgments

The authors thank Paleo Data, Inc. for their provision of the nannofossil slides. We also thank the University of South Alabama's Honors College (formerly Honors Program) and USA Foundation for funding this project. This paper is dedicated to the memory of Dr. Michael V. Doran.

Literature Cited

Anthonissen, D.E. and J.G. Ogg. 2012. Appendix 3: Cenozoic and Cretaceous biochronology of planktonic foraminifera and calcareous nannofossils. In: F.M. Gradstein, J.G. Ogg, M.D. Schmitz, and G.M. Ogg, eds. The Geologic Time Scale. Elsevier, Kidlington, Oxford, UK, p. 1083—1127. https://doi.org/10.1016/C2011—1—08249—8

Bergen, J. 1984. Calcareous nannoplankton from Deep Sea Drilling Project Leg 78A: Evidence for imbricate underthrusting at the Lesser Antillian active margin. In: S. Orlofsky, ed. Initial Reports of the Deep Sea Drilling Project, Volume 78A. U.S. Government. Printing Office, Washington, D.C., USA, p. 411—434. https://doi.org/10.2973/dsdp.proc.78a.120.1984

Blum, M.D., K.T. Milliken, M.A. Pecha, J.W. Snedden, B.C. Frederick, and W.E. Galloway. 2017. Detrital—zircon records of Cenomanian, Paleocene, and Oligocene Gulf of Mexico drainage integration and sediment routing: Implications for scales of basin—floor fans. Geosphere 13:2169–2205. https://doi.org/10.1130/GES01410.1

BOEM (Bureau of Ocean Energy Management). 2000. Outer Continental Shelf Official Protraction Diagram for Mississippi Canyon NH 16—10. United States Department of the Interior, Washington, D.C., USA. https://www.boem.gov/sites/default/files/oil—and—gas—energy—program/Mapping—and—Data/Gulf—PDFs/nh16—10.pdf

BOEM (Bureau of Ocean Energy Management). 2014. Outer Continental Shelf Official Protraction Diagram for Alaminos Canyon NG 15—04. United States Department of the Interior, Washington, D.C., USA. https://www.boem.gov/sites/default/files/oil—and—gas—energy—program/Mapping—and—Data/Gulf—PDFs/NG—15—04.pdf

Bouma, A.H., W.R. Bryant, and J.W. Antoine. 1968. Origin and configuration of Alaminos Canyon, northwestern Gulf of Mexico. Gulf Coast Association of Geological Societies Transactions 18:290—296. https://archives.datapages.com/data/gcags/data/018/018001/0290.htm

Bown, P.R. 2005. Palaeogene calcareous nannofossils from the Kilwa and Lindi areas of coastal Tanzania (Tanzania Drilling Project 2003—4). Journal of Nannoplankton Research 27:21—95. https://doi.org/10.58998/jnr2031

Browning, E., J.A. Bergen, S.A. Blair, T.M. Boesiger, and E. de Kaenel. 2017. Late Miocene to Late Pliocene taxonomy and stratigraphy of the genus *Discoaster* in the circum North Atlantic Basin: Gulf of Mexico and ODP Leg 154. Journal of Nannoplankton Research 37:189—214. https://doi.org/10.58998/jnr2037

Bukry, D. 1971. *Discoaster* evolutionary trends. Micropaleontology 17:43—52. https://doi.org/10.2307/1485036

Fulthorpe, C.S., W.E. Galloway, J.W. Snedden, P.E. Ganey—Curry, and T.L. Whiteaker. 2014. New insights into Cenozoic depositional systems of the Gulf of Mexico Basin. Gulf Coast Association of Geological Societies Transactions 64:119—129.

Galloway, W.E., P.E. Ganey—Curry, X. Li, and R.T. Buffler. 2000. Cenozoic depositional history of the Gulf of Mexico basin. American Association of Petroleum Geologists Bulletin 84:1743—1774. https://doi.org/10.1306/8626C37F—173B—11D7—8645000102C1865D

Goodwin, R.H. and D.B. Prior. 1989. Geometry and depositional sequences of the Mississippi Canyon, Gulf of Mexico. Journal of Sedimentary Research 59:318—329. https://doi.org/10.1306/212F8F85—2B24—11D7—8648000102C1865D

Haq, B.U. 1998. Calcareous nannoplankton. In: B.U Haq and A. Boersma, eds. Introduction to Marine Micropaleontology, 2nd ed. Elsevier Science (Singapore) Pte Ltd., Singapore, Singapore, p. 79—107. https://doi.org/10.1016/B978—0—444—82672—5.X5000—4

Hart, P.E., D.R. Hutchinson, J. Gardner, R.S. Carney, and D. Fornari. 2008. A photographic and acoustic transect across two deep—water seafloor mounds, Mississippi Canyon, northern Gulf of Mexico. Marine and Petroleum Geology 25:969–976. https://doi.org/10.1016/j.marpetgeo.2008.01.020

Hay, W.W. 1970. Calcareous nannofossils from cores recovered on DSDP Leg 4. In: R.G. Bader, R.D. Gerard, W.E. Benson, H.M. Bolli, W.W. Hay, W.T. Rothwell, Jr., M.H. Ruef, W.R. Riedel, and F.L. Sayles, eds. Initial Reports of the Deep Sea Drilling Project, Vol. 4. U.S. Government Printing Office, Washington, D.C., USA, p. 455—503. http://doi.org/10.2973/dsdp.proc.4.123.1970

Hay, W.W., H.P. Mohler, and M.E. Wade. 1966. Calcareous nannofossils from Nal'chik (northwest Caucasus). Eclogae Geologicae Helvetiae 59:379—399. https://doi.org/10.5169/seals—163378

Martini, E. and M.N. Bramlette. 1963. Calcareous nannoplankton from the experimental Mohole drilling. Journal of Paleontology 37:845—855.

Paleo Data ®, Inc. 2017. Biostratigraphic Chart — Gulf Basin, USA Quaternary and Neogene. Ver. 1701, 16 January 2017. Compiled by: A.S. Waterman, R.D. Weber, Y. Lu, V.E. Smith, R.A. George, T.M. Reilly, R.V. Roederer, J.A. Edmunds, B.W. Parker, N.R. Myers, A.J. Avery. Biostratigraphic chart available from https://www.paleodata.com/chart/ (viewed on 10/4/2023).

Poag, C.W. 2015. Benthic Foraminifera of the Gulf of Mexico: Distribution, Ecology, Paleoecology. Texas A&M University Press, Corpus Christi, TX, USA, 239 p.

Ross, C.B., W.D. Gardner, M.J. Richardson, and V.L. Asper. 2009. Currents and sediment transport in the Mississippi Canyon and effects of Hurricane Georges. Continental Shelf Research 29:1384—1396. https://doi.org/10.1016/j.csr.2009.03.002

Salomon, R. 1999. The Calcite Palace. https://ina.tmsoc.org/galleries/CalcitePalace/index.htm. (viewed on 10/04/2023).

Theodoridis, S. 1984. Calcareous nannofossil biozonation of the Miocene and revision of the helicoliths and discoasters. Utrecht micropaleontological bulletins 32:1—271.

Uchupi, E. 1975. Physiography of the Gulf of Mexico and Caribbean Sea. In: A.E.M. Nairn and F.G. Stehli, eds. The Ocean Basins and Margins, Vol. 3: The Gulf of Mexico and the Ca-

ribbean. Plenum Press, New York, NY, USA, p. 1–64. https://doi.org/10.1007/978–1–4684–8535–6

Xu, J., J.W. Snedden, D.F. Stockli, C.S. Fulthorpe, and W.E. Galloway. 2017. Early Miocene continental–scale sediment supply to the Gulf of Mexico Basin based on detrital zircon analysis. GSA Bulletin 129:3–22. https://doi.org/10.1130/B31465.1

Young, J.R. 1998. Neogene. In: P.R. Bown, ed. Calcareous Nannofossil Biostratigraphy, 1st ed. Springer Science+Business Media, New York, NY, USA, p. 225–265.